Article

Supramolecular Chemistry in the Structure Direction of Microporous Materials from Aromatic Structure-Directing Agents

Luis Go#mez-Hortigu#ela, Fernando Lo#pez-Arbeloa, Furio Cora#, and Joaquín Pe#rez-Pariente

J. Am. Chem. Soc., **2008**, 130 (40), 13274-13284 • DOI: 10.1021/ja8023725 • Publication Date (Web): 13 September 2008

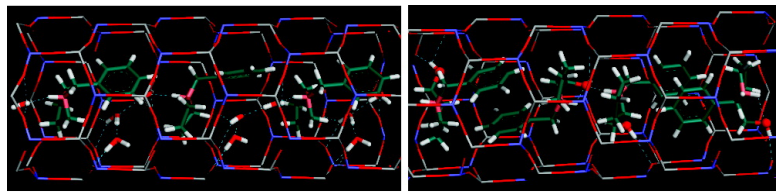

Bp: (monomer + water) occlusion **BPM: dimer occlusion**

J|A|C|S
ARTICLES

Published on Web 09/13/2008

Supramolecular Chemistry in the Structure Direction of Microporous Materials from Aromatic Structure-Directing Agents

Luis Gómez-Hortigüela,*,†,‡ Fernando López-Arbeloa,§ Furio Corà,‡ and Joaquín Pérez-Pariente†

Instituto de Catálisis y Petroleoquímica, C/ Marie Curie 2, 28049 Cantoblanco, Madrid, Spain, Davy Faraday Research Laboratory, Department of Chemistry, Third Floor, Kathleen Lonsdale Building, University College London, Gower Street, WC1E 6BT London, United Kingdom, and Departamento de Química Física, Universidad del País Vasco-EHU, Apartado 644, 48080 Bilbao, Spain

Received April 3, 2008; E-mail: lhortiguela@icp.csic.es

Abstract: A combination of fluorescence spectroscopy, thermogravimetric analysis, and molecular mechanics calculations has been used to study the structure-directing effect of the aromatic benzylpyrrolidine (BP) molecule (and its monofluorinated derivatives), and (*S*)-(−)-*N*-benzylpyrrolidine-2-methanol (BPM) in the synthesis of the microporous AFI structure. The results clearly show that, while all molecules form supramolecular aggregates in concentrated water solution, BPM molecules have a much more pronounced trend to aggregate as dimers within the AFI structure due to the development of interdimer H-bond interactions. Instead, BP (and its ortho- and meta-fluorinated derivatives) SDAs tend to incorporate in the AFI structure as monomers but with the simultaneous occlusion of water molecules, while para-fluorinated BP derivatives do not form compact dimers able to be accommodated in the AFI structure. We propose a crystallization mechanism where the presence of dimers is required for the nucleation step to occur, while crystal growth takes place through the simultaneous occlusion of SDA monomers and water (when the synthesis is performed with BP and derivatives) or through the occlusion of SDA dimers (in the synthesis with BPM).

1. Introduction

Microporous materials have been widely employed industrially in molecular sieving and ion-exchange applications,[1−3] which exploit the molecular dimensions and the crystalline nature of the microporous structure to discriminate between molecules with very subtle steric differences. In addition, many different atoms can be incorporated within the framework of these crystalline microporous solids, giving place to a range of materials with different compositions, several of which have useful catalytic properties. Since the discovery of microporous aluminophosphates ($AlPO_4$) by Wilson et al. in 1982,[4] the synthesis of these materials has been widely studied, yielding a diversity of structural types comparable to that of the previously known aluminosilicate-based zeolites.[5] In these $AlPO_4$ materials, there is a strict alternation of Al^{3+} and P^{5+} ions; nevertheless, both ions can be isomorphically replaced by heteroatoms, giving rise to acid, redox, and even bifunctional properties. Known microporous $AlPO_4$ structures include not only polymorphs that are common to both SiO_2 and $AlPO_4$ compositions but also structures that have no zeolitic counterpart.

The synthesis of microporous materials is based on hydrothermal methods, where the source of the inorganic ions, water, and generally, an organic molecule are heated in an autoclave for a time ranging from few hours to weeks.[6−8] The inclusion of the organic molecules is usually required to direct the crystallization of a certain microporous structure, and so they are called structure-directing agents (SDAs). The role of these organic molecules has been often described as a "template effect"[9] to indicate that the organic molecules organize the inorganic tetrahedral units into a particular topology around themselves during the nucleation process, providing the initial building blocks from which crystallization of the microporous structures will take place. Nevertheless, the exact role of the SDA molecules during the crystallization of microporous materials is still not fully understood,[10] and thus its study is a major issue in molecular sieves science. Controlling this feature would enable the synthesis of new topologies as well as to gain control over crystal size and morphology and the location of heteroatoms, if present. Although a true templating effect has

† Instituto de Catálisis y Petroleoquímica.
‡ University College London.
§ Universidad del País Vasco-EHU.

(1) Davis, M. E. *Acc. Chem. Res.* **1993**, *26*, 111.
(2) Naber, J. E.; de Jong, K. P.; Stork, W. H. J.; Kuipers, H. P. C. E.; Post, M. F. M. *Stud. Surf. Sci. Catal.* **1994**, *84C*, 2197.
(3) Venuto, P. B. *Microporous Mesoporous Mater.* **1994**, *2*, 297.
(4) Wilson, S. T.; Lok, B. M.; Flanigen, E. M. U.S. Patent 4,310,440, 1982.
(5) http://www.iza-structure.org/databases.
(6) Lok, B. M.; Cannan, T. R.; Messina, C. A. *Zeolites* **1983**, *3*, 282.
(7) Davis, M. E.; Lobo, R. F. *Chem. Mater.* **1992**, *4*, 756.
(8) Zones, S. I.; Nakagawa, Y.; Lee, G. S.; Chen, C. Y.; Yuen, L. T. *Microporous Mesoporous Mater.* **1998**, *21*, 199.
(9) Gies, H.; Marler, B. *Zeolites* **1992**, *12*, 42.
(10) Lobo, R. F.; Zones, S. I.; Davis, M. E. *J. Inclusion Phenom. Mol. Recognit. Chem.* **1995**, *21*, 47.

10.1021/ja8023725 CCC: $40.75

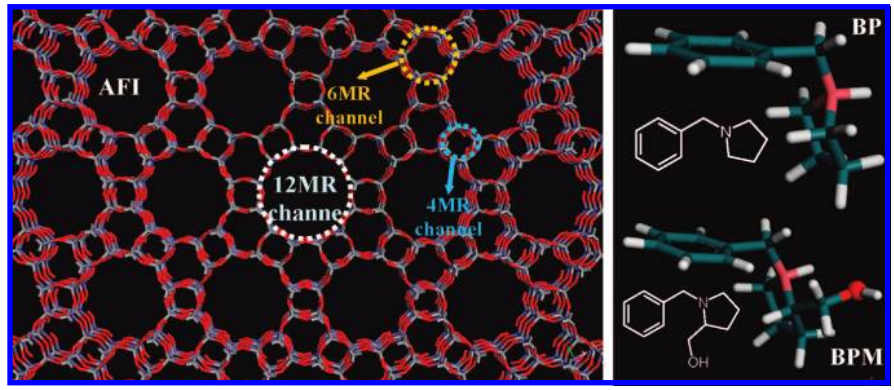

Figure 1. (Left) AFI structure, viewed perpendicularly to the channel direction, showing the different channels. (Right) molecular structures of benzylpyrrolidinium (BP: top) and (*S*)-(−)-*N*-benzylpyrrolidinium-2-methanol (BPM: bottom; oxygen atom displayed as a ball).

been occasionally found (the most common example is the triquaternary ammonium cation inside the ZSM-18 zeolite,[11]) the structure-directing effect of organic molecules is not as specific as one could expect. Experimental evidence collected along the years clearly shows that the gel chemistry and kinetic factors can also have a critical bearing on the nature of the microporous material formed.

The organic SDA molecules are encapsulated within the nascent microporous structure during its crystallization, developing strong nonbonded interactions with the framework and thus contributing to the final stability of the system. To be efficient SDAs, organic molecules are required to be moderately hydrophobic,[12] be soluble in the synthesis media (but not interact strongly with the solvent), be moderately rigid (in order to increase selectivity in structure direction), have high hydrothermal stability, and develop strong nonbonded interactions with the microporous structure within which they will be occluded. In the search for new large-pore microporous structures, increasingly larger and more complex SDAs have been gradually used, leading to the discovery of a number of new zeolitic topologies (see, for example, reference 13 to account for the molecular complexity of new SDAs).

Despite the large number of SDAs of very different sizes and shapes used up to date, their choice as structure-directing agents has almost invariably considered the features of single molecular units. The synthesis of large-pore microporous materials has been sought with the use of SDAs with larger molecular size. Supramolecular chemistry has only rarely been mentioned in the structure-direction environment, in contrast to the wide use of, for example, supramolecular micellar arrangements in the synthesis of mesoporous materials.[14] In this context, a new concept in structure direction of microporous materials has been recently proposed by us[15−17] and by Corma et al.,[18] consisting in the use of supramolecular self-assembled molecules as structure-directing agents. An example of this new concept of structure direction can be achieved using aromatic molecules that self-assemble with their aromatic rings parallel to each other through $\pi-\pi$ type interactions, being this supramolecular entity the actual structure-directing agent of the microporous structure. This new concept of structure direction permits the use of relatively simple molecules with suitable size, rigidity, thermal stability, and hydrophobicity properties to create larger and more complex zeolitic topologies due to their supramolecular aggregation. Although the aggregation of aromatic probe molecules (like for example naphthalene, anthracene, pyrene, or thionin) within zeolite structures has been demonstrated by photophysical studies after the incorporation of the aromatic molecules in postsynthetic treatments,[19−23] this concept of self-assembly has not yet been applied to the structure direction of organic molecules during the crystallization of microporous materials.

In previous works, we observed that benzylpyrrolidine (BP, Figure 1 (top, right)) and (*S*)-(−)-*N*-benzylpyrrolidine-2-methanol (BPM, Figure 1 (bottom, right)) are able to direct the crystallization of the aluminophosphate AlPO-5 (AFI-type structure).[24,25] The AFI microporous structure is composed of one-dimensional 12-membered ring (MR) channels with a diameter of 7.3 Å, which are surrounded by smaller one-dimensional 4- and 6-MR channels,[5] as illustrated in Figure 1 (left). The stability of self-assembled aggregates of these and related molecules[15−17] occluded inside the AFI-structure has been computationally demonstrated. Indeed, the BPM SDA molecule was rationally designed in an attempt to achieve a supramolecular helicoidal (and hence, chiral) arrangement of the SDA molecules within the AFI structure, promoted by its ability to self-assemble into dimers.[17] Although we had indirect experimental evidence concerning the formation of these aggregates such as the organic content occluded in the AlPO-5 samples, no direct experimental evidence of the supramolecular chemistry is still available. In this work, we present a combined experimental study based on fluorescence spectroscopy and thermogravimetric analyses, complemented with a computational

(11) Lawton, S. L.; Rohrbaugh, W. J. *Science* **1990**, *247*, 1319.
(12) Kubota, Y.; Helmkamp, M. M.; Zones, S. I.; Davis, M. E. *Microporous Mater.* **1996**, *6*, 213.
(13) Zones, S. I.; Hwang, S.-J.; Elomari, S.; Ogino, I.; Davis, M. E.; Burton, A. W. C. R. *Chimie* **2005**, *8*, 267.
(14) Cheng, C.-G.; Luan, Z.; Klinowski, J. *Langmuir* **1995**, *11*, 2815.
(15) Gómez-Hortigüela, L.; Corà, F.; Catlow, C. R. A.; Pérez-Pariente, J. *J. Am. Chem. Soc.* **2004**, *126*, 12097.
(16) Gómez-Hortigüela, L.; Pérez-Pariente, J.; Corà, F.; Catlow, C. R. A.; Blasco, T. *J. Phys. Chem. B* **2005**, *109*, 21539.
(17) Gómez-Hortigüela, L.; Corà, F.; Catlow, C. R. A.; Pérez-Pariente, J. *Phys. Chem. Chem. Phys.* **2006**, *8*, 486.
(18) Corma, A.; Rey, F.; Rius, J.; Sabater, M. J.; Valencia, S. *Nature* **2004**, *431*, 287.
(19) Suib, S. L.; Kostapapas, A. *J. Am. Chem. Soc.* **1984**, *106*, 7705.
(20) Ramamurthy, V.; Sanderson, D. R.; Eaton, D. F. *J. Am. Chem. Soc.* **1993**, *115*, 10438.
(21) Ramamurthy, V.; Sanderson, D. R.; Eaton, D. F. *J. Phys. Chem.* **1993**, *97*, 13380.
(22) Hashimoto, S.; Ikuta, S.; Asahi, T.; Masuhara, H. *Langmuir* **1998**, *14*, 4284.
(23) Thomas, K. J.; Sunoj, R. B.; Chandrasekhar, J.; Ramamurthy, V. *Langmuir* **2000**, *16*, 4912.
(24) Gómez-Hortigüela, L.; Pérez-Pariente, J.; Blasco, T. *Microporous Mesoporous Mater.* **2005**, *78*, 189.
(25) Gómez-Hortigüela, L.; Pérez-Pariente, J.; Blasco, T. *Microporous Mesoporous Mater.* **2007**, *100*, 55.

study, in order to unambiguously demonstrate the occurrence of the self-assembly of the these SDA molecules first in the synthesis gels and then within the AFI structure synthesized using these molecules as SDAs. For completeness, we also consider the monofluorinated derivatives of BP.

The present work consisted of several steps: first, the aggregation behavior of the molecules in aqueous solution was studied at different concentrations; then, AlPO-5 samples with different loadings of organic BP or BPM molecules were obtained by a series of adsorption experiments and studied by fluorescence spectroscopy in order to assign the different emission bands to the distinct aggregation states. Once assigned the bands, the state of the molecules occluded during crystallization was studied by fluorescence spectroscopy and thermogravimetric analyses; aggregation in the synthesis gels has also been studied. Finally, a computational study was performed in order to understand the experimental observations. On the basis of these results, we propose a tentative mechanism for the structure direction of these aromatic molecules in the synthesis of the AFI structure that accounts for all our observations.

2. Experimental and Computational Details

Details of the synthesis and characterization of the organic molecules employed in this study, benzylpyrrolidine (BP) (and the fluorinated derivatives) and (*S*)-(−)-*N*-benzylpyrrolidine-2-methanol (BPM), have been given elsewhere.[24,25] Aqueous solutions of BP and BPM molecules were prepared by adding equimolar amounts of the corresponding organic amine and HCl. In this way, 10^{-4}, 10^{-3}, 10^{-2}, 10^{-1}, and 1 M aqueous solutions of benzylpyrrolidinium chloride and (*S*)-(−)-*N*-benzylpyrrolidinium-2-methanol chloride were obtained and studied by fluorescence spectroscopy.

The syntheses of AlPO-5 by using BP (and fluorinated derivatives) and BPM as SDAs have also been detailed in previous works.[24,25] Synthesis gels were prepared with molar composition of 1 R:1 Al_2O_3:1 P_2O_5:40 H_2O, where R stands for the organic molecule. The gels were introduced into 60 mL Teflon lined stainless steel autoclaves and heated statically at 150 °C for 72 h. The resulting solids were separated by filtration, washed with ethanol and water and dried at 60 °C overnight. For the experiments involving the adsorption of the organic molecules BP and BPM, AlPO-5 samples were obtained by using triethylamine (TEA) as SDA, in the same molar composition as before. The use of TEA as SDA ensures that no BP or BPM molecules are present in the AFI samples prior to adsorption.

The solid samples of the synthesis gels were prepared by filtering the gels (after mixing of all the components, prior to the heating step) and drying the solid material at 60 °C overnight. The amorphous nature of these solids was evidenced by the absence of diffractions in the XRD patterns.

Calcination of the AlPO-5 sample obtained with TEA as SDA was carried out by heating the sample at 500 °C under an inert atmosphere of N_2 for 1 h, followed by 5 h at the same temperature under an oxidant O_2 atmosphere. Complete removal of the organic molecule was assessed by TGA.

Adsorption of BP and BPM was carried out in vapor phase, after an activation stage. The calcined AlPO-5 sample (obtained with TEA as SDA) was preheated at 200 °C for 2 h under a N_2 stream (N_2 flow ∼ 80 mL/min) to eliminate all the adsorbed water (TGA showed that no water remained adsorbed in the AFI structure at this temperature). During the adsorption experiments, the temperature of the AFI sample was maintained at 200 °C in order to ensure the non-adsorption of water. Then, for the adsorption of the organic molecules, the N_2 stream was bubbled through a vessel containing a liquid sample of the corresponding molecule (BP or BPM); the organic molecules were thus carried to the AlPO-5 sample in the N_2 stream. The amount of organic molecule adsorbed within the AFI structure was controlled by adjusting both the temperature of the liquid sample and the time of adsorption. The maximum temperature at which the molecule samples were heated during contact with the N_2 stream was 80 °C. After adsorption of the organic molecule for the corresponding time, the AFI samples were kept at 200 °C under the N_2 stream (without passing through the organic-containing vessel) for 2 h in order to remove the organic that could be adsorbed on the external surfaces of the AlPO-5 material.

The crystallization of the AFI structure as a pure phase, as well as its resistance to the calcination and adsorption treatments, was assessed by X-Ray diffraction (Seifert XRD 3000P diffractometer, Cu Kα radiation). The organic content of the samples was studied by chemical CHN analysis (Perkin-Elmer 2400 CHN analyzer) and thermogravimetric analysis (TGA) (Perkin-Elmer TGA7 instrument). Prior to the thermogravimetric analysis, samples were kept for 24 h under an atmosphere with a controlled humidity (∼33%) in order to completely hydrate the samples. In selected cases, the thermogravimetric analysis was performed coupled with a mass spectrometer to analyze the evolved gas (Fisons MD-800 mass spectrometer, using an ionization potential of 70 eV, with a 6 scan/min frequency and an atomic mass range of 2−200 amu).

The aggregation state of the molecules in solution and in the solid samples was studied by fluorescence spectroscopy. Liquid and solid-state UV−visible fluorescence excitation and emission spectra were recorded in a SPEX fluorimeter model Fluorolog 3-22 equipped with a double monochromator in both the excitation and the emission channels and a red-sensitive photomultiplier detector operating with a Peltier-cooling system. The fluorescence spectra were registered in the front-face configuration in which the emission signal was detected at 22.5° with respect to the excitation beam. Liquid solutions were placed in 1-mm pathway quartz cells, whereas the fluorescecence spectra of the solid aluminophosphate samples were recorded by means of thin films supported on glass slides by solvent evaporation from a dichloromethane suspension.

The computational study was based on the same protocol we developed[15−17] to rationalize the structure-directing behavior of these aromatic molecules. Molecular structures and the interaction energies of the SDAs and water with the AFI framework were described with the cvff forcefield,[26] in which van der Waals and electrostatic interactions were explicitly included. The framework atoms were kept fixed during all the calculations. Due to the very acidic pH of the synthesis gels (∼3), SDA molecules will be protonated when directing the crystallization of the AFI structure (the pK_a of BP in water at 25 °C is 9.66[27]); therefore, protonated BP and BPM amines have been studied. The atomic charges for BP (and derivatives) and BPM cations (with net molecular charge of +1) were calculated by the charge-equilibration method.[28] The SDA charge of +1 was compensated by a uniform charge background in the AFI framework.[17,29] The atomic charges for water molecules were −0.82 and +0.41 for oxygen and hydrogen, respectively, taken from the cvff parametrization, that has been shown to describe well the properties of water-containing systems.[30]

The location and interaction energies of BP (and derivatives) and BPM dimers have been discussed in previous works.[17,31] The structures were generated by loading 4 (BP and derivatives) or 24 (BPM) molecules arranged as dimers (with benzyl rings facing each other and parallel) in a 1 × 1 × 3 or 1 × 1 × 18 unit cell system

(26) Dauger-Osguthorpe, P.; Roberts, V. A.; Osguthorpe, D. J.; Wolff, J.; Genest, M.; Hagler, A. T. *Proteins: Struct., Funct., Genet.* **1988**, *4*, 21.
(27) Teitel'baum, A. B.; Kudryavtseva, L. A.; Bel'skii, V. E.; Ivanov, B. E. *Russ. Chem. B.* **1980**, *29*, 1571.
(28) Rappe, A. K.; Goddard, W. A., III. *J. Phys. Chem.* **1995**, *95*, 3358.
(29) Gómez-Hortigüela, L.; Corà, F.; Catlow, C. R. A.; Blasco, T.; Pérez-Pariente, J. *Stud. Surf. Sci. Catal.* **2005**, *158*, 327.
(30) Williams, J. J.; Smith, C. W.; Evans, K. E.; Lethbridge, Z. A. D.; Walton, R. I. *Chem. Mater.* **2007**, *19*, 2423.
(31) Gómez-Hortigüela, L.; Corà, F.; Pérez-Pariente, J. *Microporous Mesorpous Mater.* **2008**, *109*, 494.

Table 1. Weight Percentage of Organic Molecules within the AFI Structure after Adsorption or Synthesis[a]

sample	Ads-1	Ads-2	Ads-3	synthesis
AlPO-BP	1.19 (0.1)	5.20 (0.6)	9.79 (1.0)	9.81 (1.0)
AlPO-BPM	traces	1.79 (0.2)	7.90 (0.7)	12.83 (1.2)

[a] Conditions for adsorption were: Ads-1: 16 min with SDA sample at 35 °C; Ads-2: 1 h (BP) or 3 h (BPM) with SDA sample at 80 °C; Ads-3: 24 h with SDA sample at 80 °C. Values in molecules per unit cell are given in brackets.

of the AFI structure, respectively, and the most stable location was obtained by simulated annealing followed by energy minimization. The very large cell in the BPM system is required to enable the stable relative orientation between adjacent dimers, which is long-range ordered. To study the location of the SDA molecules in monomeric form, 2 molecules were manually loaded in the required orientation in a $1 \times 1 \times 2$ unit cell system of the AFI structure, and geometry optimized. Water molecules were inserted in the 12 MR channel of the AFI structure using a Monte Carlo (MC) docking procedure, where Coulombic interactions were explicitly included. Loading of water molecules was fixed to 2, 4 or 6 molecules in the 12 MR channel (1, 2 or 3 water per SDA molecule) (Note: water molecules in the 6 MR channel were explicitly excluded from the calculations since no difference was observed between the SDAs). In these calculations, the coordinates of both the AFI structure and the organic molecules were kept fixed; 10^5 configurations were sampled. The final location and interaction energies of the SDAs and water within the AFI structure were obtained by simulated annealing followed by energy minimization, where both the SDAs and the water molecules were allowed to relax. The total interaction energies were calculated by subtracting the energy of the isolated SDA and water molecules from the energy of the total system.

3. Results

We shall present results in different sections, starting from the fluorescence data on BP and BPM SDA molecules in aqueous solutions, followed by the fluorescence study of the SDAs adsorbed in the AFI structure, then of the SDAs occluded in the amorphous material of the synthesis gel and in the AFI structure during crystallization. Finally, the computational results will be presented.

Hereafter, the AlPO-5 samples will be named making reference to the molecule occluded (BP for benzylpyrrolidine, and oFBP, mFBP and pFBP for the ortho-, meta- and para-fluorinated derivatives, respectively, and BPM for (*S*)-(−)-*N*-benzylpyrrolidine-2-methanol) and the treatment for the occlusion of the SDA molecules ("ads" for adsorption or "syn" for synthesis); for "ads" samples, a number will be added at the end indicating the amount of organic loaded, in increasing order (i.e., "1" for the lowest amount and "3" for the highest one; see Table 1 for values).

3.1. SDA Molecules in Solution. Fluorescence emission spectra of the aqueous SDA solutions at different concentrations are given in Figure 2. The spectra for BP (left) and BPM (right) are very similar. At concentrations up to 10^{-2} M, only one fluorescence band centered at 282 nm is observed, that is assigned to the emission from BP and BPM monomers due to the low concentration at which this band predominates. However, an increase of the concentration to 10^{-1} M leads to the appearance of a shoulder at higher wavelengths, and at the highest concentration of 1 M, which is the concentration of organic molecules in a typical AlPO synthesis gel, this fluorescence band centered at 322 nm clearly predominates, although the band at 282 nm is still present as a small shoulder. The occurrence of this new band at 322 nm with the increase in the concentration of the molecules led us to assign it to the fluorescent emission from SDA molecules in an aggregated state, probably dimers. We can therefore conclude that these SDA molecules are arranged in supramolecular aggregates at the concentration at which the crystallization of the microporous material takes place. The fluorescence spectrum of pure BP presents an emission band at even higher wavelengths (around 355 nm), probably due to a higher interaction between the benzyl rings owing to the formation of higher-order aggregates or a closer distance between the interacting benzyl rings.

3.2. Occlusion of SDA Molecules within the AFI Structure by Adsorption. Different amounts of the organic SDAs BP or BPM were loaded in the AlPO-5 material through adsorption experiments, as detailed in the Experimental Section. The structural integrity of the AFI structure after the adsorption experiments was assessed by XRD. The amount of organic loaded could be controlled by varying both the time of adsorption and/or the temperature of the molecule sample, as can be seen in the Supporting Information (Figure 1-SI). The different amounts of organic molecules that were adsorbed in the AFI structure are given in Table 1, while the TGA data are shown in Figure 3. The high-temperature desorption of the organic molecules adsorbed in the samples is evidence that the organic molecules were occluded within the channels of the AFI structure rather than adsorbed on the external surface. The maximum amount of BP that was able to be loaded in the AFI structure was the same as the amount that is occluded during crystallization. However, this is not the case for BPM, where only 0.7 BPM molecules per unit cell could be adsorbed rather than 1.2 that were occluded during crystallization; an increase of the adsorption time to 72 h did not lead to a higher BPM loading, evidencing that the maximum BPM loading under our experimental conditions had been reached. This difference in the adsorption of the two molecules is due to their different boiling point: BP has a lower boiling point, and thus the amount of BP that the N_2 stream carries during the adsorption experiments is higher.

Fluorescence emission spectra of AlPO-5 samples loaded with different amounts of BP and BPM after adsorption are shown in Figure 4. For samples loaded with BP, it can be clearly observed that, at low SDA concentrations (0.1 and 0.6 BP molecules per unit cell), a band centered at 288 nm predominates, that can be directly assigned to BP molecules occluded within the AFI structure as monomers. A band at around double the wavelength of the monomer emission (~560 nm) appears when this is very intense; this band comes from the uncorrected second-order effect of the emission monochromator for the fluorescent emission from the monomers (hereafter called second-order emission). However, the monomer emission is accompanied by another broader band in the range between 400 and 500 nm that becomes predominant when the SDA concentration is increased to 1.0 BP molecules per unit cell. The high wavelength of this band and its concentration dependence led us to assign this band to BP in aggregated states within the AFI structure. In this case, due to the confinement effect provided by the occlusion within the AFI structure, only dimer aggregates can be located within the channels, so we can unambiguously assign this band to BP dimers. The band corresponding to the BP dimers within the AFI structure is much more red-shifted with respect to the monomer than in solution; this shift could be due to the confinement effect, i. e. the interaction of the aromatic rings with the channel walls, but also to a stronger $\pi-\pi$ interaction between the aromatic rings

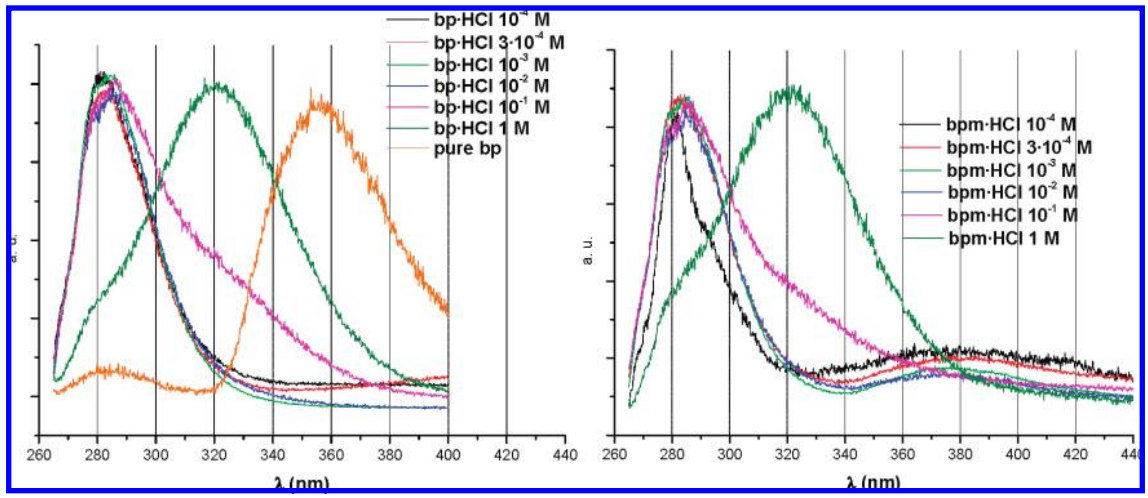

Figure 2. Height-normalized fluorescence emission spectra of benzylpyrrolidinium chloride (left) and (*S*)-(−)-*N*-benzylpyrrolidinium-2-methanol chloride (right) aqueous solutions at different concentrations. The fluorescence emission spectrum of pure liquid benzylpyrrolidine is also shown (left). The excitation wavelength was 260 nm.

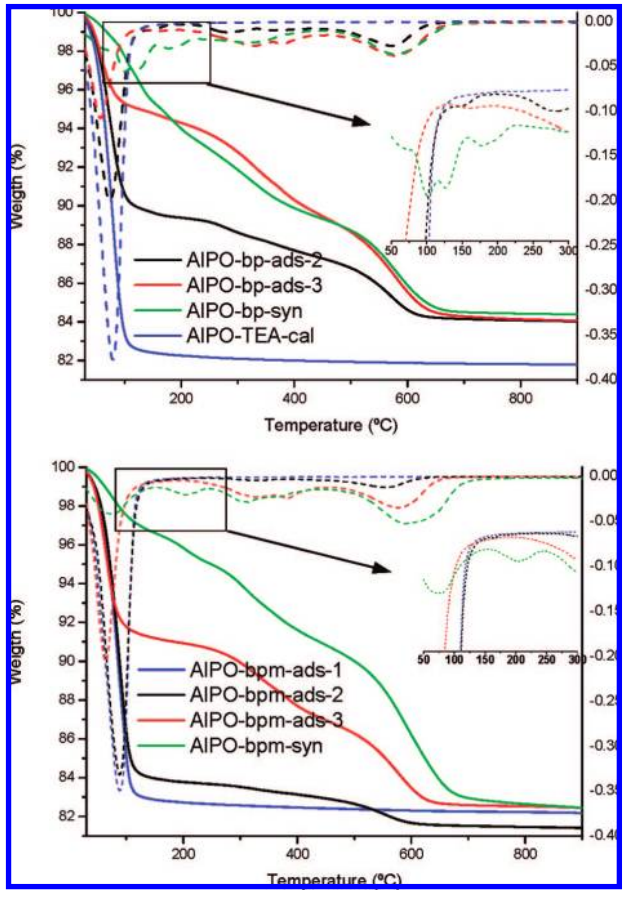

Figure 3. TGA (solid lines) and DTA (dashed lines) in air of AlPO-5 samples with occluded BP (top) or BPM (bottom) after adsorption (with different amounts of organic loaded) or synthesis. AlPO-5 calcined sample (obtained with TEA as SDA) is also shown (top). Inset: Enlarged DTA highlighting the water desorption temperature range.

in the dimers due to a closer distance (computational results show that indeed the distance between aromatic rings in BP dimers inside the AFI structure is shorter than it is in solution).

In contrast, only the band in the range between 400 and 500 nm can be observed for AlPO samples loaded with BPM, even at the lowest concentration. These results evidence that, although

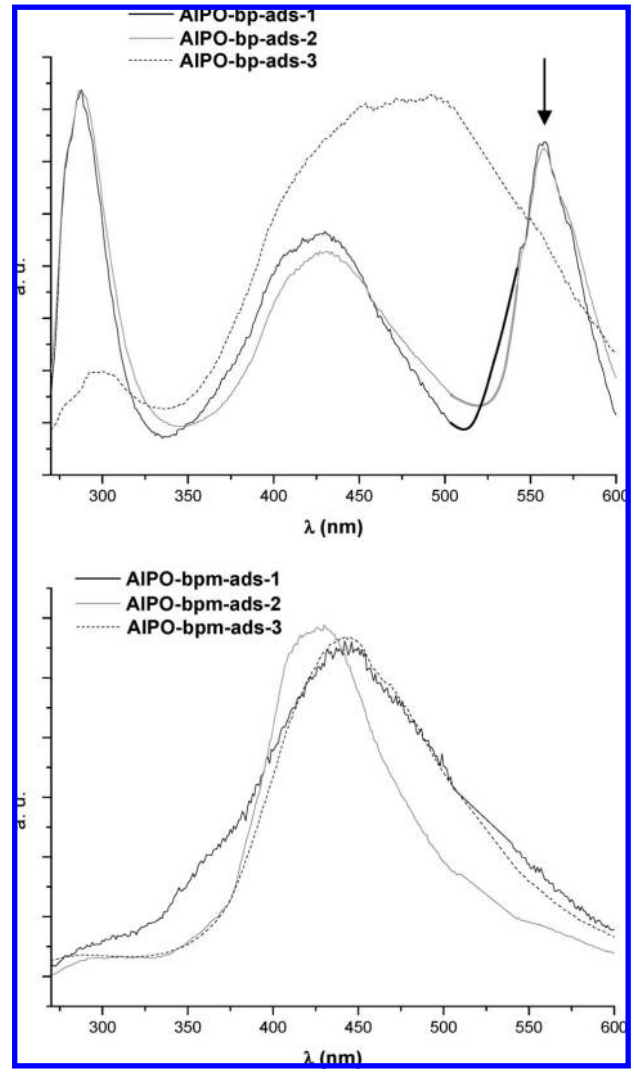

Figure 4. Height-normalized fluorescence emission spectra of solid-state AlPO-5 samples after adsorption of BP (top) or BPM (bottom). The excitation wavelength was 260 nm. A very intense signal coming from the first harmonic of the excitation wavelength observed at 520 nm has been manually removed (range between 510 and 540 nm). The arrow indicates the second-order emission from the monomer.

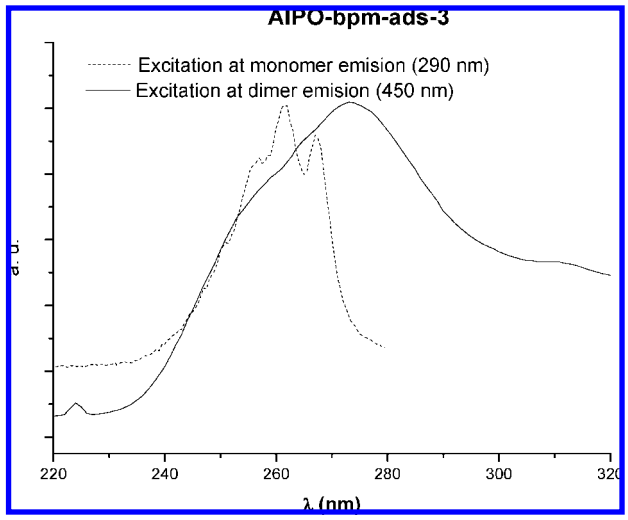

Figure 5. Height-normalized fluorescence excitation spectra of solid-state AlPO-BPM-ads-3 sample, monitored at the monomer (290 nm: dashed line) and at the dimer (440 nm: solid line) emission wavelengths.

both molecules are able to arrange as dimers when occluded inside the AFI channels, this trend is much more pronounced in the BPM molecule, where all the molecules, even at very low concentrations, are present in the form of dimers.

In order to verify that the assigned dimer emission does not come from the formation of a dynamic excimer, i.e. a dimer in the excited state, the excitation spectra for the monomer and dimer emissions were recorded (monitoring the emission at 290 and 440 nm, respectively). Results for sample AlPO-BPM-ads-3 are shown in Figure 5, where it can be clearly observed that the excitation peak maxima are shifted from 261 (monitoring at monomer emission) to 273 nm (monitoring at dimer emission). These differences in the two excitation spectra demonstrate the existence of the dimer associated in the ground state.[19,23]

Results presented in this section provide therefore the fluorescence fingerprints for the monomeric and dimeric forms of BP and BPM within the AFI structure; the characteristic fluorescent emission bands appear at ∼280 nm for the monomer and in the range between 400 and 500 nm for the dimer. These data will be applied to the analysis of AFI synthesized with BP and BPM molecules.

3.3. Aggregation of the SDA Molecules in the Synthesis Gel. The fluorescence emission spectra discussed in the previous sections enable us to use this technique to characterize the incorporation of BP and BPM molecules in the AFI structure during crystallization. Aggregation of the molecules was studied in the synthesis gels, as a previous step to the crystallization of the AFI structure. Fluorescence emission spectra for the solid samples of the synthesis gels with BP and BPM, prepared as detailed in the Experimental Section, are shown in Figure 6. It can be clearly observed that both the monomeric and the dimeric species are present in the synthesis gels in both cases; nevertheless, a slightly higher concentration of the dimer can be observed for the BPM molecule. Bands at ∼560 nm come from the second-order monomer emission. These results will be discussed in detail in the Discussion section.

3.4. Occlusion of SDA Molecules within the AFI Structure during Crystallization. Both BP and BPM molecules were able to efficiently direct the crystallization of the AFI structure, as was demonstrated by XRD,[24,25] without notable differences, except for a small increase of the c lattice parameter (channel

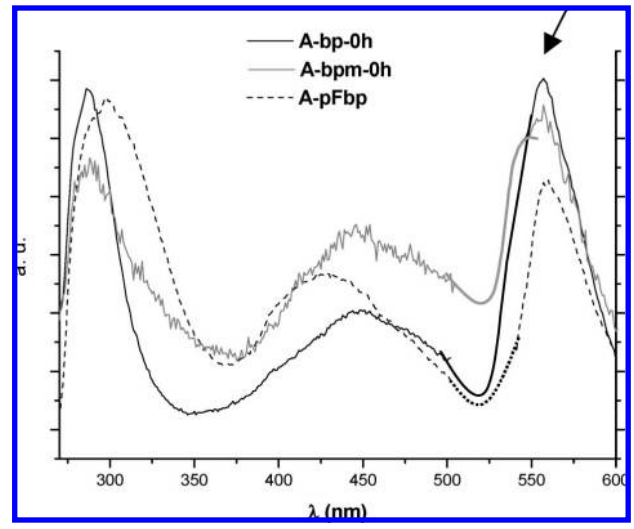

Figure 6. Height-normalized fluorescence emission spectra of AlPO gels (solid samples before heating) obtained with BP (solid black line) and BPM (solid gray line) as SDAs, and of sample obtained with pFBP after 72 h of heating at 150 °C (dashed black line). The excitation wavelength was 260 nm. A very intense signal coming from the first harmonic of the excitation wavelength observed at 520 nm has been manually removed (range between 500 and 540 nm). The arrow indicates the second-order emission from the monomer.

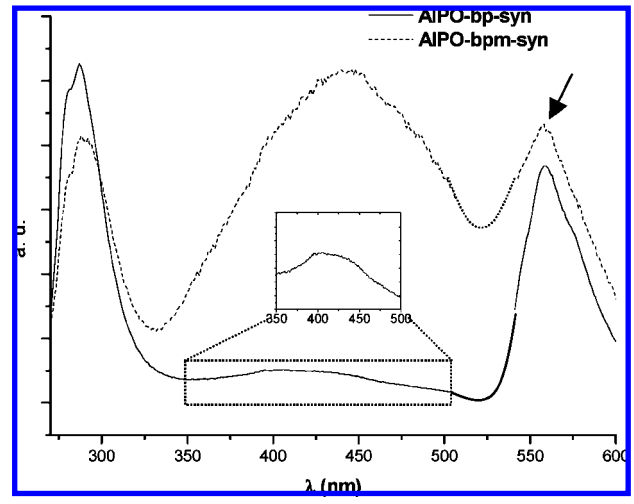

Figure 7. Height-normalized fluorescence emission spectra of solid-state AlPO-5 samples crystallized with BP (solid line) and BPM (dashed line) as SDAs. The excitation wavelength was 260 nm. A very intense signal coming from the first harmonic of the excitation wavelength observed at 520 nm has been manually removed (range between 500 and 540 nm). The arrow indicates the second-order emission from the monomer. Inset: enlargement of dimer emission in the AlPO-BP-syn sample.

direction) observed for the material synthesized using BPM (8.41 Å for BP versus 8.45 Å for BPM). TGA, elemental CHN analysis and ^{13}C-MAS NMR demonstrated the resistance of both molecules to the hydrothermal treatment and their integral incorporation within the AFI structure.

Fluorescence emission spectra of AFI solid samples synthesized with BP and BPM are shown in Figure 7. The spectra show that monomer emission predominates for BP occluded during crystallization of the AFI structure, although the emission from the dimer can also be observed. However, the opposite is found for BPM, where the dimer emission is predominant. Again, bands at around 560 nm come from the second-order monomer emission. These results indicate that, although both

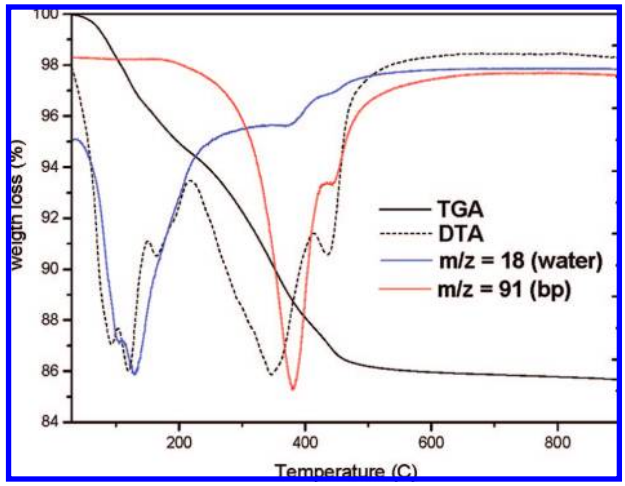

Figure 8. TGA (black solid line) and DTA (black dashed line) under helium atmosphere of AlPO-BP-syn sample. Desorption of water ($m/z = 18$, blue solid line) and BP ($m/z = 91$, $PhCH_2^+$, red solid line) are monitored by mass spectrometry of the evolved gases.

the dimer and the monomer aggregation states are present in the two cases, most BP molecules are occluded within the AFI structure as monomers, while most BPM are as dimers. Such a higher trend for BPM to arrange as dimers was also found for the samples in which the SDAs were occluded in the AFI structure by adsorption, and to a lesser extent, in the synthesis gels.

The organic and water contents inside the AFI structure were analyzed by elemental CHN analysis and TGA. Results from elemental analysis indicate that 9.3 wt % of BP and 13.2 wt % of BPM are occluded during the crystallization of the AFI structure, that correspond to 1.0 BP and 1.2 BPM molecules per AFI unit cell. TGA of the AlPO-BP-syn sample showed a strong desorption at temperatures between 100 and 220 °C, which did not appear for AlPO-BP-ads samples obtained by adsorption (Figure 3-top-inset). This desorption cannot correspond to release of water adsorbed on the external surface of the material or occluded in the 6 MR channels of the AFI structure since the same should appear in the AlPO-BP-ads samples (and also in the calcined AlPO-5-TEA sample). Desorption of the latter water molecules is expected to occur at temperatures below 100 °C, as is the case for all AlPO-BP-ads and calcined AlPO-5-TEA samples; indeed, this desorption can be observed for AlPO-BP-syn sample at temperatures below 100 °C. TGA coupled to mass spectroscopy analysis was then applied to the AlPO-BP-syn sample in order to identify the nature of the chemical species desorbed in the 100−220 °C range. The results (Figure 8) led us to unambiguously assign the desorption in the 100−220 °C temperature range to the release of water molecules, since desorption of BP molecules starts at temperatures above 200 °C. However, such a high desorption temperature for water suggests that those water molecules are somehow retained within the AFI structure, possibly entangled between the BP molecules and the AFI channel walls.

In contrast, a different behavior is observed for the AlPO-BPM-syn sample (Figure 3 (bottom-inset)). While a clear water desorption can be observed at temperatures below 100 °C, corresponding to water occluded in the 6 MR channels and/or adsorbed on the external surface, a much less intense water desorption is observed in this case in the temperature range between 100 and 220 °C.

A rough estimation of the water content (water release was considered at temperatures up to 220 °C), based on these results and earlier computational works[32] where it was observed that 4 water molecules per unit cell can be accommodated within the 6 MR channels of the AFI structure, indicates that 1.0 BP and around 6.2 water molecules per AFI unit cell are loaded in the AlPO-BP-syn sample; 4 of these water molecules would be located in the 6 MR channels and 2.2 would be occluded in the 12 MR channels within the organic BP molecules (4 MR channels are too small to accommodate water). Meanwhile, 1.2 BPM and around 4.5 water molecules per AFI unit cell are loaded in the AlPO-BPM-syn sample, corresponding to 4 water molecules in the 6 MR channels and 0.5 in the 12 MR channel.

The values obtained for the water content in the 12 MR channel within the organic SDAs, together with the lower trend for BP SDA to arrange as dimers within the AFI structure shown by fluorescence spectroscopy, suggest that during crystallization of the AFI structure, BP is preferentially occluded as monomers but accompanied by occlusion of water (2−3 water molecules per BP), while BPM is occluded as dimers and with no simultaneous occlusion of water.

Let us now consider the monofluorinated BP molecules. In previous works[24] we demonstrated that the meta-fluorinated derivative of BP (mFBP) was more efficient than BP in directing the crystallization of the AFI structure, while the ortho-derivative (oFBP) was less efficient, although was still able to direct it. We measured the fluorescence spectra of AlPO-5 samples obtained with these fluorinated SDAs to complete the study, and we observed a higher concentration of monomeric SDAs compared to dimers, as occurs for the nonfluorinated derivative (BP) (Figure S-2 in the Supporting Information). However, a higher concentration of dimers in the AlPO-5 sample obtained with mFBP was observed compared to that of BP, which was accompanied by a slightly higher organic loading (1.1 mFBP molecules per unit cell, as measured by TGA). Instead, the para-fluorinated derivative did not direct the crystallization of the AFI structure, but only led to amorphous material;[24] this issue will be discussed below, in the Discussion section.

3.5. Computational Study. A computational study based on molecular mechanics was performed in order to explain the experimental observations discussed in the previous section. The monomer configuration was studied by locating the molecules with benzyl rings in opposite sides (see Figure 9 (left)), and loading different amounts of water molecules through MC simulations in the 12 MR channels. For the dimer configuration, the molecules were located with benzyl rings in the same side, facing and overlapping each other (see Figure 9 (right)); in this arrangement, no water molecules could be loaded in the 12 MR channel by MC simulations due to the lack of void space. The most stable location and the interaction energies were obtained by relaxing the SDA and water molecules via simulated annealing followed by energy minimization.

The energy results and the final locations for each arrangement are given in Table 2 and Figure 9, respectively. We observe that the most stable arrangement for BP corresponds to the monomer configuration with the simultaneous occlusion of three water molecules per SDA. A similar behavior is found for the meta- and ortho-fluorinated derivatives of BP, where the highest interaction is reached through the simultaneous occlusion of monomers and water. However, the opposite is found for

(32) Gómez-Hortigüela, L.; Corà, F.; Márquez-Álvarez, C.; Pérez-Pariente, J. *Chem. Mater.* **2008**, *20*, 987.

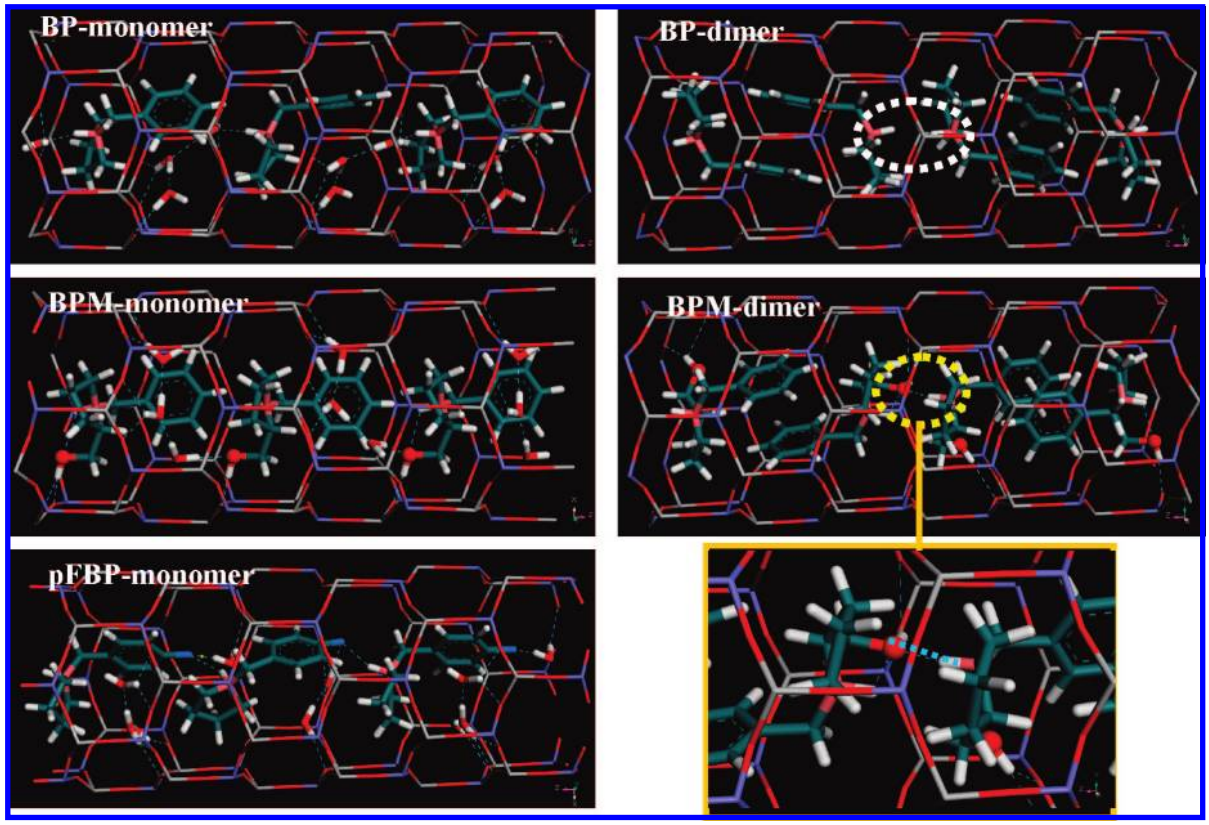

Figure 9. Most stable location of BP (top) and BPM (middle) molecules arranged as monomers (left, with 3 water molecules per SDA) and dimers (right, with no water molecules). (Bottom: left) most stable location of pFBP molecules arranged as monomers with 3 water molecules per SDA; (bottom: right) enlargement of the interdimer H-bond developed between consecutive BPM dimers. Nitrogen, carbon, fluorine and oxygen atoms are displayed in pink, green, blue and red, respectively. Oxygen atoms in the CH_2OH moiety in BPM are displayed as balls. The white and the yellow circles highlight the interdimer N^+-N^+ repulsion in BP and the interdimer H-bond between consecutive BPM dimers, respectively.

Table 2. Interaction Energy (in kcal/mol per unit cell) of the Different Molecular Arrangements and with Different Water Contents[a]

Aggregation SDA/u.c.	Monomer: 1.0 SDA				Dimer: 1.33 SDA
Water/u.c.	0	1	2	3	0
AlPO-BPM	−136.8	−149.9	−168.0	−182.5	**−194.7**
AlPO-BP	−130.0	−142.0	−157.5	**−175.9**	−173.6
AlPO-mFBP	–	–	–	**−181.6**	−176.5
AlPO-oFBP	–	–	–	**−178.8**	−170.2
AlPO-pFBP	–	–	–	−189.4	–

[a] The most stable arrangements for each molecule are highlighted in bold. The interaction energies for the fluorinated derivatives of BP are also given.

the BPM molecule, where the most stable arrangement clearly corresponds to the dimer configuration; in this case, no inclusion of water is possible in the 12 MR channels as dimers provide very efficient space filling in the 12 MR channels. These results can effectively rationalize the experimental findings, and demonstrate the preference of BPM to arrange as dimers in the AFI channels.

4. Discussion

The combination of experimental and computational results evidences a higher trend for BPM compared to BP to arrange as dimers when occluded within the AFI structure, both upon adsorption in postsynthetic treatments or during structure direction in the crystallization process. The slight increase of the c lattice parameter of the unit cell obtained with BPM as SDA may be associated with the dimeric form of the organic molecule, which has larger effective size than the monomer. However, no difference in the aggregation behavior is observed in water solution, where it was found that both molecules are mostly present in their aggregated state at the concentration typical of the synthesis gels. This distinct supramolecular chemical behavior in the two media suggests that the different tendency of BP and BPM to aggregate is particular to the occlusion of the molecules within the microporous AFI material, i.e. to its confinement effect.

For both molecules, we observed that the dimer configuration is more abundant when the molecules are incorporated in the AFI structure by adsorption. One possible explanation for this could be the lack of water during the adsorption experiments, since water can compete with the dimer inclusion, especially in hydrophilic frameworks like AlPOs. However, it could also be due to a different protonation state of the molecules: during crystallization, SDA molecules are expected to be protonated (the pK_a of BP in water at 25 °C is 9.66) due to the low pH of the synthesis gel (∼3), while during adsorption molecules are more likely to be in neutral state. The close location of the nitrogen atoms of SDA molecules in adjacent dimers in the AFI channel would cause an electrostatic repulsion between consecutive dimers (Figure 9, (top right), dashed white circle) that destabilizes the dimer configuration; this dimer instability would be especially true if the molecules are protonated, as is the case in the synthesis, decreasing their trend to arrange as dimers.

On the other hand, the different aggregation behavior of BP and BPM cannot be only due to the preference of BP to simultaneously incorporate water molecules within the AFI

structure since the same behavior was found in the samples where the SDAs were loaded by adsorption, where no water molecules are present. Indeed, BPM has a more hydrophilic nature compared to BP due to the presence of the methanol ($-CH_2OH$) group. We would therefore expect a stronger simultaneous occlusion of water in the case of BPM. However, this is not the case; BPM molecules arrange preferentially as dimers within the AFI structure. The driving force for the preferential dimerization of BPM in contrast to BP can be explained in terms of, first, the higher interaction of BPM with the AFI structure due to the presence of the methanol ($-CH_2OH$) group, that strongly interacts with the channel walls through the development of H-bonds with the framework oxygens. This increased interaction drives the system to incorporate as many BPM molecules as possible, as can be achieved via the occlusion of the molecules as dimers since in this configuration ~1.3 molecules rather than 1.0 (as monomers) are loaded per AFI unit cell. Second, the presence of the hydroxyl group enables the development of intermolecular H-bonds between NH and OH functional groups of consecutive dimers, as shown in Figure 9 (bottom right), thus stabilizing the dimer configuration and compensating for the electrostatic repulsion between ammonium groups.

A similar picture as for BP is found when AFI samples synthesized using the meta- and ortho-fluorinated derivatives of BP are studied. These molecules are also preferentially incorporated as monomers with the simultaneous occlusion of water, in agreement with the interaction energy results. Nevertheless, the concentration of mFBP dimers, although still not predominant with respect to the monomer, is slightly higher than that for BP. This increased dimer presence, together with the higher interaction (both in the monomer and dimer configurations), could explain its higher efficiency to direct the crystallization of the AFI structure (compared to BP).

Our results suggest therefore a different supramolecular chemistry of the BP and BPM types of molecules during structure direction of the AFI structure. The structure-directing effect of BP takes place through the simultaneous occlusion of BP as monomer and water molecules (around 3 per BP molecule) in a "cooperative" structure-directing effect, while BPM structure-directs the AFI structure through the occlusion of dimers. Such a different behavior should be reflected in the crystallization rates obtained using the two SDAs. Kinetic experiments (Figure S-3 in the Supporting Information) showed a higher crystallization rate for BPM (crystallinity was 75 and 100% after 1 and 3 h heating) since these molecules stack and form compact dimers within the AFI structure (whose dimensions are similar) rather than being occluded as isolated monomers, as is the case for BP (crystallinity was respectively 60 and 93% after 1 and 3 h), indirectly confirming our hypothesis.

The presence of a certain amount of BP dimers in AlPO-BP-syn sample has been evidenced by fluorescence spectroscopy. This result may suggest that the dimer configuration is required, at least for a nucleation role, during the crystallization of the AFI structure. We demonstrated in previous works[15,24] that the para-fluorinated derivative of BP (pFBP) is not able to direct the crystallization of the AFI structure since pFBP molecules cannot arrange as dimers when occluded within the 12 MR channels of the AFI structure; this is due to an intermolecular repulsion provoked by the presence of the fluorine atoms. The interaction energy for the pFBP SDA occluded within the AFI structure as monomers with three water molecules per SDA, calculated in the same way as before, was found to be −189.4 kcal/mol per u. c., evidencing an even higher interaction with the framework than for BP and even mFBP monomers (−175.9 and −181.6 kcal/mol, respectively, see Table 2). Such a high interaction energy is due to stabilizing interactions through H-bonds between F atoms and NH groups of pFBP consecutive monomer molecules, as can be seen in Figure 9 (bottom left). Therefore, if SDA monomers could by themselves direct the crystallization of the AFI structure, pFBP molecules should be able to direct it even more efficiently than BP and mFBP, since they have a more favorable interaction with the framework (pFBP monomers are present in the synthesis gel, as will be evidenced below in Figure 6). However, we experimentally observed that pFBP does not lead to the crystallization of the AFI structure.[24] These observations strongly suggest that, at least in a small amount, the presence of dimers (able to be occluded within the AFI structure) is required to make viable the crystallization of the AFI structure, possibly during the nucleation stage. Indeed, the shape and dimensions of dimers are very similar to those of the cylindrical 12 MR AFI channels, while those for monomers are not, suggesting that the presence of dimers is required for templating the initial AFI nuclei. Energy results for oFBP also support this hypothesis, as oFBP monomers develop a higher interaction energy than BP monomers, but experimentally they are less efficient in directing the AFI structure; indeed, the interaction of oFBP dimers with the AFI structure is the lowest. This hypothesis would also be in agreement with the results from the kinetic experiments, where the higher crystallization rate observed for BPM would be explained as well by the fact that BPM dimers are more easily formed and thus the nucleation rate is enhanced.

In an attempt to provide further evidence for the necessity of dimers to initiate the crystallization of the AFI structure, fluorescence spectra of the synthesis gels (before heating) were recorded (Figure 6). Results clearly demonstrate that dimers of both BP and BPM SDAs are present in the synthesis gels; in fact, BP dimers are much more abundant in the gel than inside the AFI structure. Therefore, nucleation of the microporous structure might involve a reorganization (condensation) of the TO_4 units surrounding the SDA dimers toward the cylindrical shape of the 12 MR AFI channels. The fluorescence spectrum of the sample obtained with pFBP (where no AlPO-5 structure was crystallized) was also measured (Figure 6). Since this sample did not lead to the crystallization of the AFI structure, but only to amorphous material, it should be reminiscent of the structure of the gel; it was observed that pFBP dimers were also formed in this amorphous solid. However, these pFBP dimers cannot direct the crystallization toward the AFI structure, as experimentally evidenced. This lack of structure direction might be due to the fact that, although the benzyl rings can locate (stack) parallel to each other in the gel, which is the form required to originate a dimer-like band in the fluorescence spectrum, the presence of fluorine in para-position prevents the pyrrolidine rings to bend inward. We expect therefore the pFBP dimers to have a less compact conformation, with the pyrrolidine rings oriented outward (see Figure 10 (middle left)); fluorescence does not enable us to differentiate among different dimeric conformations. The geometry of the pFBP dimers makes them unable to fit in the cylindrical shape of the AFI structure, preventing its crystallization, as shown in Figure 10 (middle left).

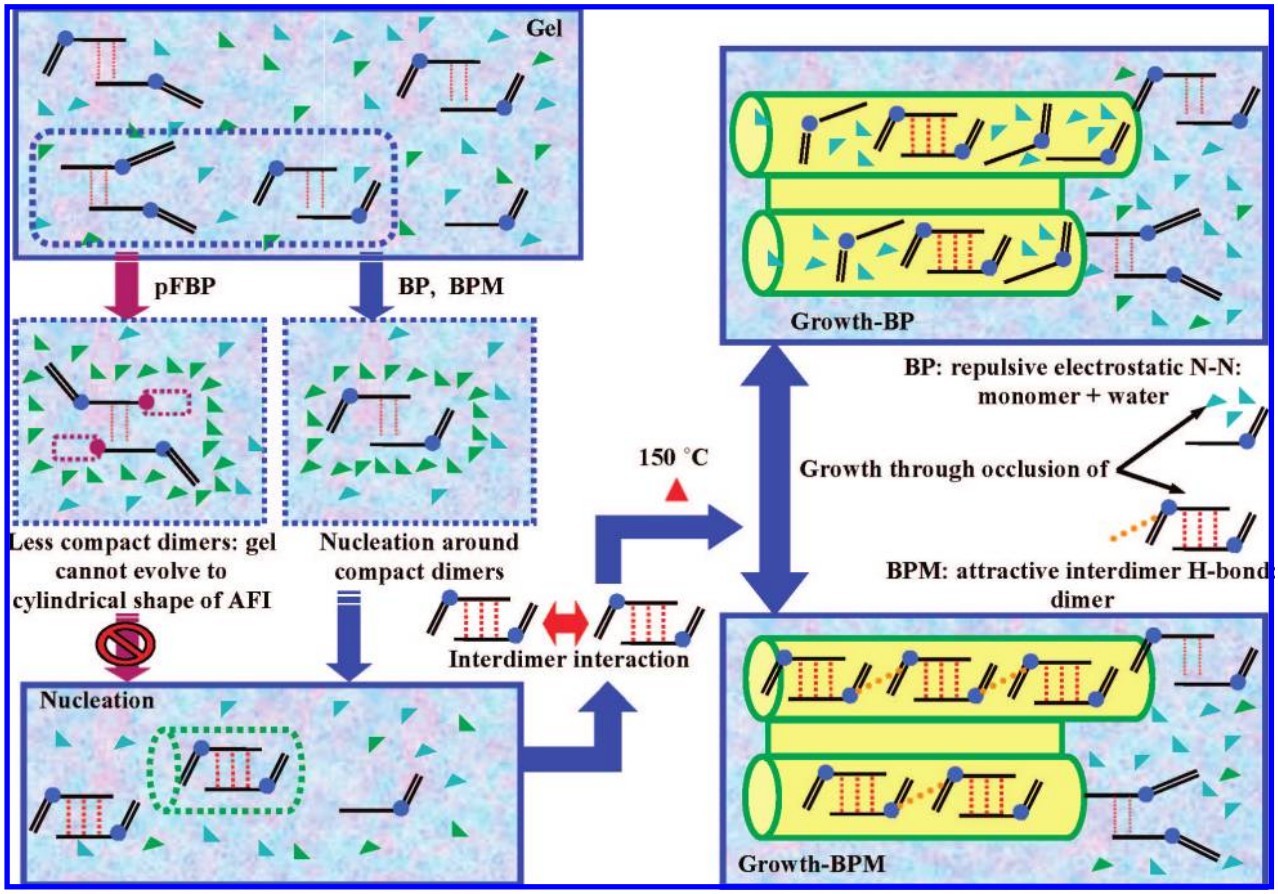

Figure 10. Schematic picture of the proposed mechanism for the crystallization of AlPO-5 from BP and BPM SDAs. The "gel" and "nucleation" steps are common for BP and BPM SDAs, but not for pFBP, whose dimers cannot evolve to the AFI structure. Once the viable nuclei are formed, depending on the repulsive (BP) or attractive (BPM) nature of the interdimer interaction, crystalline growth takes place in different ways. Phenyl rings and pyrrolidine rings are represented as thick single lines and thin double lines, respectively, while blue circles represent N atoms; purple circles denote fluorine atoms in the parafluorinated BP, and its repulsive area is shown as a purple dashed rectangle. Green triangles denote $(TO_n)_m$ units (Al and P oxide units), and blue triangles denote implicit water molecules. The AFI structure is shown as green cylinders (line is dashed in the nucleation step). Dashed red lines indicate $\pi-\pi$-type interactions, its intensity depending on the number and width of lines. Dashed orange lines indicate interdimer H-bonds in BPM. Results for oFBP and mFBP are similar to BP.

The evidence shown in this and previous works provides detailed insight into the structure-directing effect of benzyl-containing SDA molecules on the crystallization of microporous aluminophosphate materials. Although some speculative issue remains, as individual steps have not been observed experimentally, the collective information gathered enables us to formulate an atomic level mechanism for structure direction that accounts for all our present observations so far. Our proposed mechanism is depicted in Figure 10. In a first stage, both BP and BPM SDAs form aggregates in the gel under our synthesis conditions (high SDA concentration). Nucleation takes place through the aggregation of (AlO_4) and (PO_4) units (whatever the nature of these units is) around the SDA dimers: due to the good size match with the 12 MR channel geometry, the dimer units direct the nucleation step. Fluorine atoms in pFBP dimers in the gel force the pyrrolidine rings to be oriented in a less compact way, yielding a poor match between pFBP and the cylindrical shape of the 12 MR channels. Once some nuclei are viable after condensation of (AlO_4) and (PO_4) units around BP and BPM dimers, crystalline growth takes place in different ways for the two molecules: the electrostatic repulsion between charged N atoms of BP molecules in consecutive dimers forces the preferential occlusion of additional SDAs during crystal growth as BP monomers with the simultaneous occlusion of water molecules. However, the strong stabilization created by interdimer H-bonds between consecutive BPM dimers leads this system to occlude BPM dimers during the crystal growth stage. A similar picture than for BP is found for its ortho- and meta-fluorinated derivatives.

Our observations suggest therefore that the nucleation and crystal growth steps during the synthesis of a microporous material may occur through different molecular units. Indeed, Zones et al. already used this concept and proposed a new zeolite synthesis system in which a minor amount of a SDA is used to selectively specify the nucleation product, and then a larger amount of a cheaper, less selective molecule is used to provide both pore filling and basicity capacities in the synthesis as the crystal continues to grow.[33,34]

Our results in the crystallization of the large-pore AFI structure thus demonstrate the validity of our initial concept that proposed the use of self-assembled organic molecules as structure-directing agents for the synthesis of microporous materials. Benzyl-containing organic molecules, especially BPM, at the concentration used in the synthesis gels, form supramolecular aggregates via stacking of the aromatic rings, stabilized through $\pi-\pi$ interactions, and thus generating larger molecular units that originate large-pore structures. Such supramolecular

(33) Zones, S. I.; Hwang, S.-J.; Davis, M. E. *Chem. Eur. J.* **2001**, *7*, 1990.
(34) Zones, S. I.; Hwang, S.-J. *Chem. Mater.* **2002**, *14*, 313.

assembly appears to be required for the formation of the initial nuclei, although the crystal growth process is less restrictive and can occur through occlusion of supramolecular or single molecular SDA units.

Conclusions

In this work we have successfully used fluorescence spectroscopy to study the aggregation of SDA molecules within the AFI structure when they are incorporated either during the crystallization of the material or in postsynthetic treatments. We have identified different emission bands corresponding to monomeric and dimeric aggregation states and have demonstrated that both benzylpyrrolidine and (*S*)-(−)-*N*-benzylpyrrolidine-2-methanol are able to arrange as dimers within the AFI structure, although the latter shows a stronger preference for the dimeric form.

The fluorescence spectroscopy results, together with thermogravimetric analysis complemented with molecular mechanics calculations, showed that the most stable mechanism of incorporation for benzylpyrrolidine molecules within the AFI channels during crystallization is as monomers, with the simultaneous occlusion of water (∼3 water per BP), giving place to a cooperative structure-directing effect. Structure direction of (*S*)-(−)-*N*-benzylpyrrolidine-2-methanol instead takes place through the occlusion of dimers due to the development of strong H-bond interactions between consecutive dimers. However, the dimeric arrangement seems to be required also for BP at least in the first stage of nucleation for the crystallization of the AFI structure to occur.

These results demonstrate that a rational control of the supramolecular chemistry of organic molecules can provide a new and efficient tool in the structure direction of microporous materials, and thus open new possibilities in microporous materials science, consisting in the use of self-assembled aggregates of simpler organic molecules as structure-directing agents in the synthesis; molecular aggregates could eventually lead to new framework topologies with larger pores.

Acknowledgment. Financial support of the Spanish Ministry of Education and Science (project CTQ2006-06282) is acknowledged. L.G.H. acknowledges the Spanish Ministry of Education and Science for a postdoctoral grant; F.C. is supported by an RCUK Fellowship. L.G.H. is grateful to R. Arevalo for helpful discussions. C. Márquez-Álvarez and A. Pinar are acknowledged for their help with the adsorption and synthesis experiments, respectively. We also thank Accelrys for providing their software.

Supporting Information Available: Details of the adsorption experiments of benzylpyrrolidine within the AFI structure, fluorescence spectra of AlPO-5 samples obtained with meta- and ortho-fluorinated derivatives of benzylpyrrolidine, and a study of the kinetics of crystallization of AlPO-5 structure-directed by BP and BPM. This material is available free of charge via the Internet at http://pubs/acs.org.

JA8023725